

New excited states in the halo nucleus ${}^6\text{He}$

X. Mougeot^a, V. Lapoux^{a,*}, W. Mittig^{b,1}, N. Alamanos^a, F. Auger^a, B. Avez^a, D. Beaumel^c, Y. Blumenfeld^c, R. Dayras^a, A. Drouart^a, C. Force^b, L. Gaudefroy^d, A. Gillibert^a, J. Guillot^c, H. Iwasaki^{a,1}, T. Al Kalanee^b, N. Keeley^e, L. Nalpas^a, E.C. Pollacco^a, T. Roger^b, P. Roussel-Chomaz^b, D. Suzuki^c, K.W. Kemper^f, T.J. Mertzimekis^{g,2}, A. Pakou^g, K. Rusek^e, J-A. Scarpaci^c, C. Simenel^a, I. Strojek^e, R. Wolski^{h,i}

^aCEA, Centre de Saclay, IRFU, Service de Physique Nucléaire, F-91191 Gif-sur-Yvette, France

^bGANIL, Bld. Henri Becquerel, BP 5027, F-14021 Caen Cedex, France

^cInstitut de Physique Nucléaire, CNRS-IN2P3, F-91406 Orsay, France

^dCEA, DAM, DIF, F-91297 Arpajon, France

^eDepartment of Nuclear Reactions, National Centre for Nuclear Research, PL-00681, Warsaw, Poland

^fDepartment of Physics, Florida State University, Tallahassee, Florida 32306-4350, USA

^gDepartment of Physics and HINP, University of Ioannina, GR 45110 Ioannina, Greece

^hFlerov Laboratory of Nuclear Reactions, JINR, Dubna, RU-141980, Moscow region, Russia

ⁱThe Henryk Niewodniczanski Institute of Nuclear Physics, PL-31342, Kraków, Poland

Abstract

The low-lying spectroscopy of ${}^6\text{He}$ was investigated via the 2-neutron transfer reaction $p({}^8\text{He},t)$ with the ${}^8\text{He}$ beam delivered by the SPIRAL facility at 15.4A.MeV. The light charged particles produced by the direct reactions were measured using the MUST2 Si-strip telescope array. Above the known 2^+ state, two new resonances were observed: at $E^* = 2.6 \pm 0.3$ MeV (width $\Gamma = 1.6 \pm 0.4$ MeV) and at 5.3 ± 0.3 MeV with $\Gamma = 2 \pm 1$ MeV. Through the analysis of the angular distributions, they correspond to a 2^+ state and to a $L = 1$ state, respectively. These new states, challenging the nuclear theories, could be used as benchmarks for checking the microscopic inputs of the newly improved structure models, and should trigger development of models including the treatments of both core excitation and continuum coupling effects.

Keywords: ${}^8\text{He}(p,t)$, transfer reaction, Borromean nucleus, resonant states

These last 30 years, the use of radioactive beams to produce nuclei far from the valley of stability has led to the discovery of a large variety of new phenomena, which were not expected in the nuclear structure theories tested on the stable nuclei: alpha-cluster like, halo or neutron-skin structures, low-lying resonant states have been observed in the light nuclei close to the neutron drip-line [1, 2]. The shell structure has also been found deeply modified from the picture established close to the β -stability line, with the apparition of new magic numbers [3]. These new features have been triggering intensive theoretical developments to explain the change in our usual nuclear structure conceptions. The recent highlights in our field have been the find-

ings of the role played by the three-nucleon interaction (TNI) in the nuclear spectra of the light nuclei [4] and in the drip-line location [6, 5] as well as the influence of the spin-isospin tensor term in the shell level ordering of the states [3] and the effects of the continuum-coupling (CC) between bound, resonant and scattering states in the low-lying spectra of the weakly-bound nuclei [7]. To understand the weak binding features of the light nuclei close to the drip-line, these CC effects have been investigated within various frameworks, the Gamow Shell Model (GSM) [7, 8, 9], the Continuum Shell Model CSM [10] or the Complex Scaled Cluster Orbital Shell Model (COSM) [11]. However, if these nuclear models are successful in predicting the characteristics of the ground or first well-studied excited states of the p-shell exotic nuclei, they disagree for the predictions of the other low-lying excited states. The discrepancies between theories question the validity of the

*Corresponding author

Email address: valerie.lapoux@cea.fr (V. Lapoux)

¹present address: NSCL, Michigan State University, USA

²Present address: University of Athens, Greece

microscopic inputs used for the description of the nuclear interactions, the various techniques adopted for the treatment of the many-body correlations, and their interplay with the CC effects. In this context, the low-lying spectroscopy of the light exotic nuclei represents a testing ground to constrain the models and to check their assumptions. It is the purpose of this article to present our experimental study of the low-lying positive parity excited states of the ${}^6\text{He}$ nucleus and to compare it to the predictions of the most recent nuclear theories. ${}^6\text{He}$ has neutron thresholds located at low energy ($S_n = 1.87$ and $S_{2n} = 0.97$ MeV) and no bound excited state. The first excited state is a 2^+ at 1.8 MeV ($\Gamma = 113$ keV) [12]. ${}^6\text{He}$ is now well known as a halo nucleus [13, 2] and the 2n-halo structure was intensively investigated within few-body models [14, 2], but the positions, spin and parities of the resonant states above 1.8 MeV remained to be determined. On the theoretical side, various calculations [14, 11, 4] or No-Core Shell Model (NCSM) with TNI [15], indicated that a series of 2_2^+ , 1_1^+ , 0_1^+ states should exist above the 2_1^+ state and below the triton-triton threshold S_{t+t} at 12.3 MeV, but they disagree on the energies of these states. Experimentally, the main results were obtained via transfer reactions, which indicated resonances below S_{t+t} and broad resonances above. From the ${}^7\text{Li}({}^6\text{Li}, {}^7\text{Be}){}^6\text{He}$ reaction [16], a 2^+ state was indicated at 5.6 MeV with a $\Gamma = 10.9$ MeV width and structures possibly $(1, 2)^-$ at 14.6 ($\Gamma = 7.4$) MeV, and at 23.3 ($\Gamma = 14.8$) MeV; a broad one ($\Gamma = 4$) at 4 MeV was reported in Ref. [17], and at 18 MeV ($\Gamma = 7.7$) in Ref. [18]. From the ${}^6\text{Li}(t, {}^3\text{He}){}^6\text{He}$ reaction resonance-like structures were seen at 7.7, 9.9 MeV and at 5 ($\Delta L = 1$) and 15 MeV [19]. No resonance except the 2^+ was indicated from the ${}^6\text{He}(p, p')$ scattering at 40.9A.MeV [13]. None of these experiments was successful to determine precisely the energy and width of the expected resonant states. In a recent experiment at the GANIL facility, the scattering and 1n-transfer reaction of the ${}^8\text{He}$ SPIRAL beam on proton [20] were studied. The (p, t) to the ${}^6\text{He}$ ground state (gs) and 2_1^+ excited state were also measured [21], with cross sections of the order of 1 mb/sr. This 2n transfer appeared to be a good probe to populate the possible excited states of ${}^6\text{He}$ with sufficient yields, taking advantage of the low energy and high intensity of the ${}^8\text{He}$ SPIRAL beam.

We report here the results of the (p, t) experiment carried out with the ${}^8\text{He}$ beam accelerated at 15.4A.MeV, and using an improved set-up to measure at forward angles the triton-particle correlations in the exit channel: triton with either ${}^6\text{He}$ in case of the $(p, t){}^6\text{He}_{gs}$, or with the ${}^4\text{He}$ particle produced in the decay of the excited states of the ${}^6\text{He}$ nucleus into ${}^4\text{He} + 2n$. The beam had

no contaminant, and a mean intensity of 1.8×10^4 /s. The target was a 50 μm -thick (4.48 mg/cm^2) foil of polypropylene $(\text{CH}_2)_n$. Two beam tracking detectors CATS [22] were mounted upstream of the target to reconstruct the incident trajectories on the target. The measured beam spot sizes were 4 and 5 mm (FWHM) in horizontal and vertical directions, respectively, and of the order of 0.5° (FWHM) for the angle distributions. The identification of the particles, reconstruction of the trajectory and measurement of the energies were done by combining five telescopes of the new MUST2 Si-strip array [23] at forward angles: four modules were arranged in a square wall located 15 cm downstream of the target, and the fifth one was at 30 cm. The light charged particles protons (p), deuterons (d) and tritons (t) produced by the elastic, (p, p') and 1n and 2n transfer reactions were measured in the wall, in coincidence with the ejectiles focused at forward angles in the 5th telescope placed behind a plastic scintillator. The first stage of each telescope was a 300 μm thick Si-strip detector with an active area of $10 \times 10 \text{ cm}^2$ and 128 (X, Y) strips, measuring the energy loss ΔE , the time of flight (ToF, with reference to the second CATS) and the position. The angular resolution at 15 cm from the target is 0.3° ; the energy resolution of the Si-strips is 40 keV at 5.5 MeV. The residual energy E was measured by the second stage, a 4 cm-thick CsI-crystal detector. Depending on their energies, the particles are identified using the standard correlation techniques between ΔE and ToF, and ΔE versus E [23].

The kinematical characteristics of the triton, total kinetic energy and scattering angle in laboratory (lab.) frame, were obtained event by event. By considering the events with $t+{}^6\text{He}$ or $t+\alpha$ coincidences, the ${}^8\text{He}(p, t)$ reactions were fully reconstructed, and the excitation energy (E_x) spectra of ${}^6\text{He}$ were deduced via missing mass method from the relativistic kinematics of the triton. We consider here the tritons identified in MUST2 via $E-\Delta E$. Their energies are above 11 MeV, with (p, t) kinematics corresponding to angles in the center of mass (c.m) frame from 35° up to 150° . The kinematics and the deduced E_x spectra of ${}^6\text{He}$ are presented in Fig. 1. These events were collected with a total number of 1.52×10^9 ${}^8\text{He}$. The contributions of possible α -t coincidences due to reactions on the carbon of the $(\text{CH}_2)_n$ target were measured with a pure carbon target. The analysis of the E_x spectra obtained for different angular ranges showed that the physical background due to the reactions on carbon is constant in our domain of excitation energies. It is modelled by the thick line shown in the spectra in Figs. 2-3. The physical background was also estimated. It is due to many-body kinematical effects of the pro-

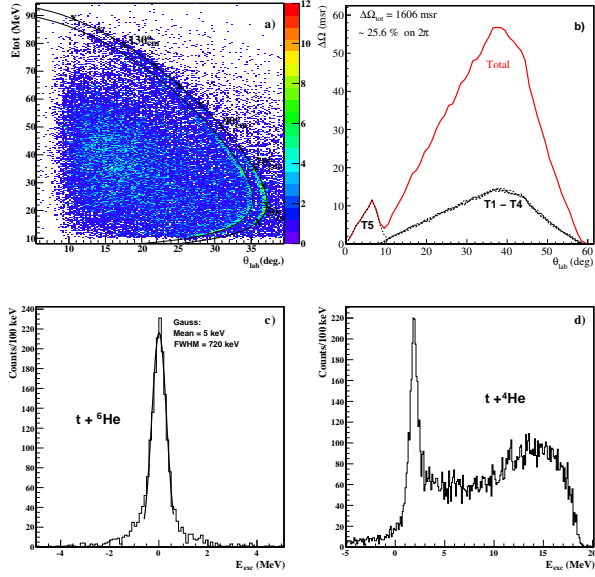


Figure 1: a) Kinematics of the tritons produced by reactions of ^8He on proton at 15.4A.MeV; they are identified via $E-\Delta E$ and correlated with α or ^6He particles. The lines are the calculated kinematics for the (p,t) reaction to the ^6He gs and 2^+ state with crosses indicating the c.m. angles for the gs by steps of 10° and starting from 40° up to 150° . The total solid angle coverage of the set-up is shown in b). Panels c) and d) are the E_x spectra of ^6He obtained from the kinematics of the triton between 35 and $150^\circ_{c.m.}$ with different conditions applied for the coincidence of triton with c) ^6He or d) ^4He .

cesses producing the same particles as the (p,t) reaction, α and t in the final state, but without involving an excited state of ^6He . Only 3 processes may contribute, corresponding to the detection of $t + \alpha$ in the final state, either with a 3-body kinematics : (i) $t + ^5\text{He} + n$ with the decay $^5\text{He} \rightarrow \alpha + n$, (ii) $t + \alpha + n^2$ with 2 correlated neutrons, or (iii) a 4-body : $t + \alpha + n + n$ with 2 uncorrelated neutrons. The main source is the contribution of the $^6\text{He}^*$ decay into $\alpha+n+n$.

We adopted the Breit-Wigner parametrization to define the distribution of a resonance with the energy E_R and intrinsic width Γ_R :

$$f(E) = \frac{1}{\pi} \frac{\Gamma_R/2}{(E - E_R)^2 + (\Gamma_R/2)^2} \cdot \quad (1)$$

The possible resonances were modelled as Breit-Wigner shapes of width Γ folded with a Gaussian function, to take into account the spreading due to the experimental resolution, estimated of the order of 610 up to 720 keV (FWHM). The known resonance 2^+_1 was obtained at 1.8(2) MeV, $\Gamma = 0.1 \pm 0.2$ MeV consistent with the literature, and then fixed in the search at 1.8 MeV with $\Gamma = 113$ keV. The parameters of the other resonances

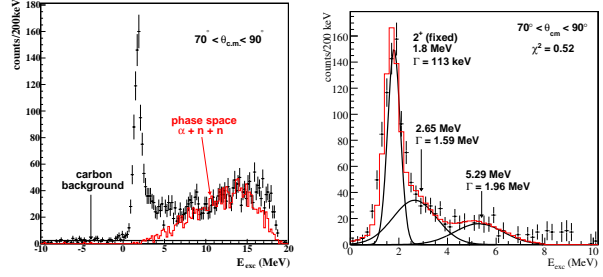


Figure 2: ^6He E_x spectrum obtained with a gate between $70-90^\circ_{c.m.}$ from the triton kinematics detected in coincidence with an α : (left part) with the components of the physical background due to the carbon content (black curve) and to the few-body processes ($\alpha+n+n$) in exit channel (red curve); (right) after subtraction of the physical background, and analysis (in the 0 to 8 MeV range) with the resonances discussed in the text.

were fitted, and the normalisation of all the peaks and resonances were free to vary.

A structure can be considered as a resonant nuclear state if its parameters (position and width) are conserved within error bars, whatever the angular slice examined. To exhibit the fit of the resonances, we first show in Fig. 2 an example of the E_x spectrum obtained for the angular range $70-90^\circ_{c.m.}$ with full statistics (left part) and analyzed after background subtraction. This operation was only the preliminary step to locate more easily the resonances, in the search range between 0 and 8 MeV. Two new possible states are indicated between 1.8 and 8 MeV. Above 8 MeV the structures are embedded in the physical background and no resonance parameter could be extracted consistently. The complete analysis, to confirm the existence of the resonances, was done by fitting the E_x spectra with the full data set (no background subtraction), for various angular slices and in the 0 to 20 MeV range, so as to take into account the effect of the physical background at high energies. The resonance parameters were extracted in a kinematical domain for which the best excitation energy resolutions are obtained (less than 720 keV FWHM) with significant statistics: between 65 and $150^\circ_{c.m.}$, the E_x spectra obtained for various small c.m. gates (range of $10^\circ_{c.m.}$) were analyzed to check the consistency of the extracted parameters of the possible resonances, and the number of these states was also varied and checked. These E_x spectra obtained by applying the c.m. gates: $[65;75]$, $[75;85]$, $[85;95]$, $[95;115]$ and $[115;150]^\circ$ are shown in Fig. 3 with the total slice for $[65;150]^\circ$. The background effects (black dotted curve in Fig. 3) are modelled with a Monte-Carlo simulation including the phase space calculations and the experimental response of the set-up.

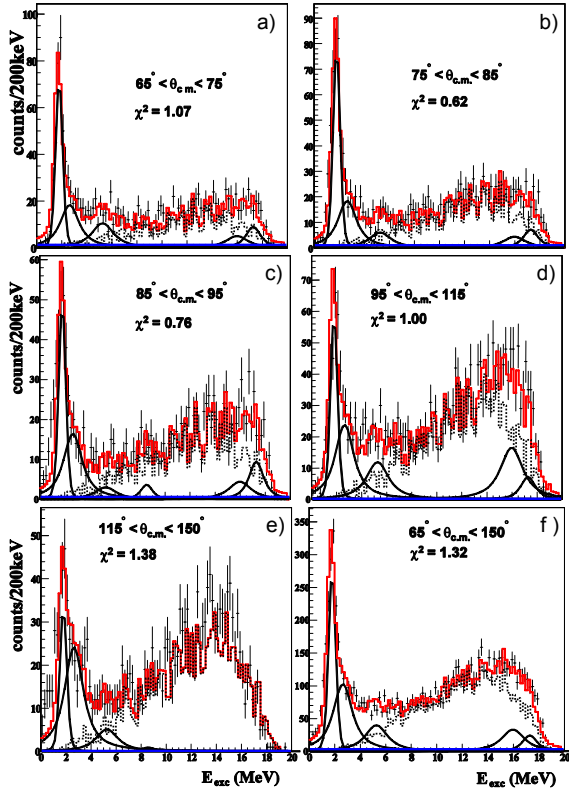


Figure 3: Analysis of the E_x spectra of ${}^6\text{He}$ obtained from $t+\alpha$ correlations and for slices of the kinematics corresponding from a) to f) to the angular ranges indicated in the frames. The data with the statistical errors are indicated with the black crosses. The final red curves are obtained by summing the background due to the carbon (blue line), the phase space (black dotted) and the resonances (solid lines).

At excitation energies above S_{t+t} , the only way to reproduce the shape of the data is to introduce two broad structures located at 16 (width 2 MeV) and 17.3 MeV (width 1.1 MeV) in addition to the phase space contributions. Being at the limit of the kinematical efficiency, their positions cannot be determined precisely. However they are consistent with the broad structures reported in previous experiments [18, 19].

The resonances in search and the total physical background contributions were included in the calculated red curve in Fig. 3. The χ^2 minimization between the data and the calculated curve was considered for the energy range between 0 and 20 MeV. A structure observed around 8 MeV was not considered as a state since it was observed for only one slice. New resonances were found: at 2.6 ± 0.3 MeV with an intrinsic width $\Gamma = 1.6 \pm 0.4$ MeV and at 5.3 ± 0.3 MeV with $\Gamma = 2 \pm 1$ MeV.

Now, considering all the events with a triton detected

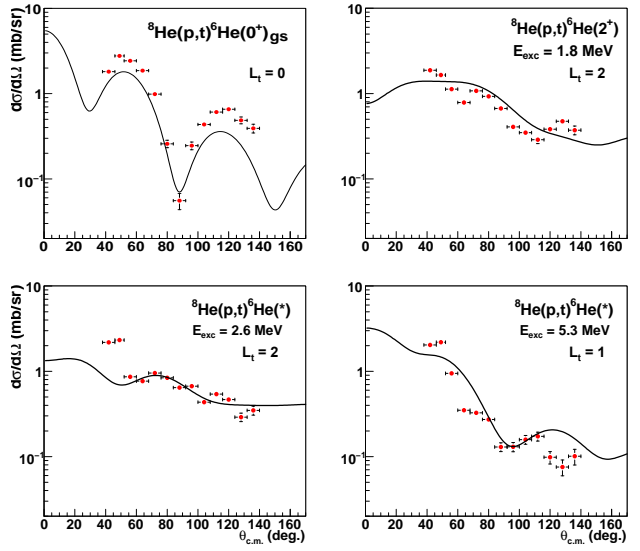


Figure 4: Experimental cross sections for ${}^8\text{He}(p,t)$ at 15.4A.MeV. The calculated curves (top panels: 2-step CRC, bottom: 1-step CRC) are described in the text.

in MUST2 and no forward coincidence, the angular distributions were deduced for the (p,t) to the gs, the known 2_1^+ and the new excited states of ${}^6\text{He}$. The statistical error is included within the points of Fig. 4. The systematical errors due to the target thickness, the normalization, the efficiency and the subtraction of the background were estimated to the level of 11% in the case of the resonant states, and 9% for the bound state in exit channel (total error bar). We have obtained distributions to the new states, and the extension of the $(p,t)0^+, 2_1^+$ up to $140^\circ_{c.m.}$. First, we compare the data for the (p,t) distributions to the gs and to the 2_1^+ state at 15.4A.MeV with the analysis done in the coupled-reaction-channel (CRC) framework. The previous data set at 15.6A.MeV was obtained only for the gs and 2_1^+ states, below $80^\circ_{c.m.}$ [20, 21]. It was described consistently within CRC calculations, the spectroscopic factors (SF) of the ${}^8\text{He}_{gs}$ with respect to ${}^7\text{He}_{3/2^-}$ -gs and ${}^6\text{He}(0^+)$ and ${}^6\text{He}(2^+)$ were extracted, the C^2S values were 2.9, 1.0 and 0.014, respectively, with error bars of the order of 30%. The agreement between the present data set and the previous CRC curves confirms the extracted SFs, and the gs structure of ${}^8\text{He}$ interpreted as a mixing between the $(1p_{3/2})^4$ and $(1p_{3/2})^2(1p_{1/2})^2$ configurations. This corroborates the $\alpha + 4n$ calculations [25] and the recent dineutron cluster structure discussed by the AMD theory [26].

Two-step CRC calculations including the new states of ${}^6\text{He}$ are needed to fully interpret the new data. This would require to complete the previous CRC framework

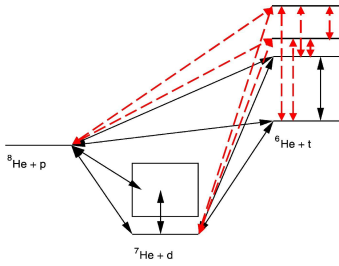


Figure 5: Schematic of the coupling scheme needed for the 2-step CRC calculations: the black lines show the channels included for the calculations of (p,t) to the gs and 2_1^+ state of ${}^6\text{He}$; the red ones are the channels required for the new states.

discussed in Ref. [21] and to include consistently the two new states as shown in Fig. 5. By comparison between the data and the calculations, the SF of the new states could be inferred. However, these calculations remain complicated due to the interplay of the new channels. The development of this framework and the extraction of the SF for the new states is in progress and will be presented in a forthcoming article [24]. Here we can simplify the analysis to deduce the transferred angular momentum L_t of the new states, by comparing the shape of the curves for various L_t values to the data. The 2 curves presented in Fig. 4 (top panels) are examples of $L_t = 0, 2$ within 2-step calculations. $L_t = 0$ can be excluded for the new states, $L_t = 2$ shape is consistent only for the 2.6 MeV state. We have also considered various L_t values for the one-step $0^+ 2n$ -pair transfer between the 0^+ gs of ${}^8\text{He}$ and the new excited states. The curves in agreement with the shape of the cross sections are given in Fig. 4: the (p,t) distribution to the 2.6 MeV state is reproduced with a $L_t=2$; this state is a 2^+ . The state at 5.3 MeV corresponds to a $L_t=1$. Of course, such limited 1-step transfer calculation can produce only the natural parity 1^- corresponding to $L_t=1$. However within 2-step processes for the (p,t), the neutrons can be transferred sequentially, and, in this future complete framework, this $L_t=1$ state may correspond to a 1^+ .

These resonances are compared to the calculations from various theoretical frameworks: the few-body model [14], the QMC using UIX and TNI (IL2 force) [4], NCSM with TNI (TM99) [15], the models treating explicitly the CC of bound and scattering states like CSM [10] and GSM [8, 9], and the Complex Scaled COSM [11]. The inclusion of TNI force which is crucial to have the correct features for the binding energy and the 2_1^+ state is not sufficient to predict correctly the other states, strongly affected by the CC. As can be seen

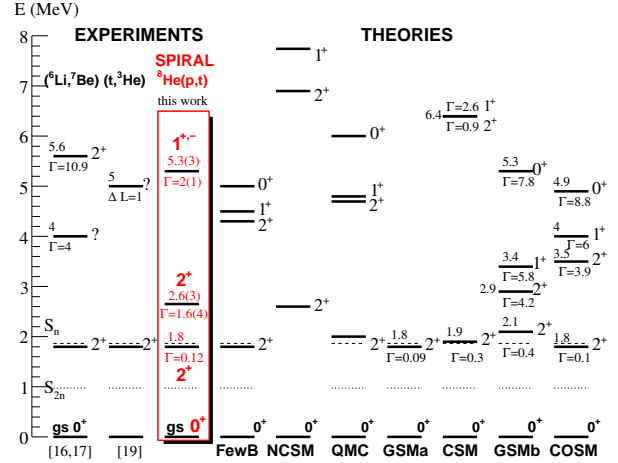


Figure 6: Spectroscopy of ${}^6\text{He}$: comparison between our new results with the previous experiments and with several theories, few-body model (FewB) [14], QMC [4], NCSM [15], CSM [10], GSMa [9], GSMb [8], and the COSM [11].

in Fig. 6, the models including the CC [8, 11] provide a better description of the 2^+ states, found closer to the gs than in the other models. The important feature of these models is their realistic treatment of the coupling to the continuum: the two neutrons of the halo can interact with each other and be excited to the continuum states. However, a complete understanding of both the position and width of the new states is not reached with the present version of the modern theories. Several effects may be needed to improve the description of ${}^6\text{He}$, such as the excitations of the ${}^4\text{He}$ core, considered as inert in most calculations. A promising approach was developed recently: the role of the particle-hole excitations of ${}^4\text{He}$ is now taken into account in the coupled-cluster calculations of ${}^6\text{He}$ states [27]. These effects may provide new interesting findings for the properties of the states located above the S_n threshold.

In conclusion, the results obtained via the ${}^8\text{He}(p,t)$ reactions are the most complete ones collected for the low-lying spectroscopy of ${}^6\text{He}$, with the evidence of two new resonances and the measurement of a whole set of angular distributions. The new states at 2.6 (3) and at 5.3 (3) MeV were found consistent with a 2^+ and an $L_t = 1$ state, respectively. They provide new constraints for the nuclear models. More generally, resonant states of the light exotic nuclei could represent benchmark data sets for the future approaches, expected to combine the treatment of the realistic interaction developed on the 3-body forces with the many-body correlations between valence nucleons and continuum effects [9].

Acknowledgments

We wish to thank the SPEG staff, P. Gangnant and J-F. Libin, and the GIP team at GANIL, for their help in the preparation of the experiment.

References

- [1] I. Tanihata *et al.*, Prog. Part. Nucl. Phys. **35**, 505 (1995).
- [2] B. Jonson, Phys. Rep. **389**, 1 (2004).
- [3] T.Otsuka *et al.*, Phys. Rev. Lett. **87**, 082502 (2001), *ibid* **95** 232502 (2005).
- [4] S.C. Pieper, R.B. Wiringa, and J. Carlson, Phys. Rev. C **70**, 054325 (2004).
- [5] T. Otsuka *et al.*, Phys. Rev. Lett. **105** 032501, (2010).
- [6] G. Hagen *et al.*, Phys. Rev. C **80**, 021306 (2009).
- [7] N. Michel, W. Nazarewicz, M. Płoszajczak and K. Bennaceur, Phys. Rev. Lett. **89**, 042502 (2002); Phys. Rev. C **67**, 054311 (2003).
- [8] G. Hagen, M. Hjorth-Jensen, J.S. Vaagen, Phys. Rev. C **71**, 044314 (2005).
- [9] N. Michel, W. Nazarewicz and M. Płoszajczak, Phys. Rev. C **82**, 044315 (2010).
- [10] A. Volya, V. Zelevinsky, Phys. Rev. Lett. **94**, 052501 (2005).
- [11] T. Myo, K. Kato, K. Ikeda, Phys. Rev. C **76**, 054309 (2007).
- [12] D.R. Tilley *et al.*, Nucl. Phys. A**708**, 3 (2002).
- [13] A. Lagoyannis *et al.*, Phys. Lett. B **518**, 27 (2001).
- [14] B.V. Danilin *et al.*, Phys. Rev C **55**, 577 (1997).
- [15] P. Navrátil, W. E. Ormand, Phys. Rev. C **68**, 034305 (2003).
- [16] J. Jänecke *et al.*, Phys. Rev. C **54**, 1070 (1996).
- [17] S. Nakayama *et al.*, Phys. Rev. Lett. **85**, 262 (2000).
- [18] H. Akimune *et al.*, Phys. Rev. C **67**, 051302 (2003).
- [19] T. Nakamura *et al.*, Phys. Lett. B **493**, 209 (2000); Eur. Phys. J. A**13**, 33 (2002).
- [20] F. Skaza *et al.*, Phys. Lett. B **619**, 82 (2005); Phys. Rev. C **73**, 044301 (2006).
- [21] N. Keeley *et al.*, Phys. Lett. B **646**, 222 (2007).
- [22] S. Ottini *et al.*, NIM A **431**, 476 (1999).
- [23] E. Pollacco *et al.*, Eur. Phys. J. A **25**, 287 (2005).
- [24] X Mougeot, V. Lapoux *et al.*, to be submitted to PRC.
- [25] K. Hagino, N. Takahashi, H. Sagawa, Phys. Rev. C **77**, 054317 (2008).
- [26] Y. Kanada-En'yo, Phys. Rev. C **76**, 044323 (2007).
- [27] G. R. Jansen, M. Hjorth-Jensen, G. Hagen, and T. Papenbrock, Phys. Rev C **83**, 054306 (2011).